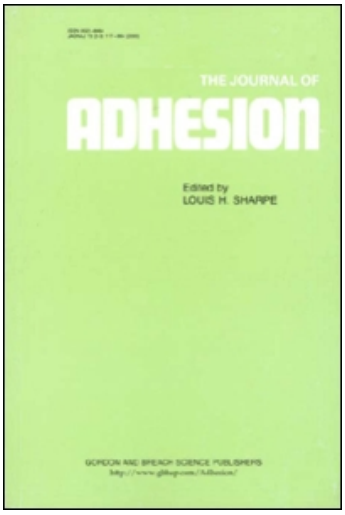

The Journal of Adhesion

Publication details, including instructions for authors and subscription information:
http://www.informaworld.com/smpp/title~content=t713453635

Surface Pretreatment of Zinc and its Adhesion to Epoxy Resins

P. J. Hine[ab]; S. El Muddarris[a]; D. E. Packha[a]
[a] School of Materials Science, University of Bath, Bath, England [b] Department of Physics, The University, Leeds

To cite this Article Hine, P. J. , Muddarris, S. El and Packha, D. E.(1984) 'Surface Pretreatment of Zinc and its Adhesion to Epoxy Resins', The Journal of Adhesion, 17: 3, 207 — 229
To link to this Article: DOI: 10.1080/00218468408074930
URL: http://dx.doi.org/10.1080/00218468408074930

J. Adhesion, 1984, Vol. 17, pp. 207–229
0021–8464/84/1703–0207 $18.50/0

Printed in the United Kingdom

Surface Pretreatment of Zinc and its Adhesion to Epoxy Resins

P. J. HINE†, S. EL MUDDARRIS and D. E. PACKHAM‡

School of Materials Science, University of Bath, Bath BA2 7AY, England.

(*Received May 24, 1984*)

An epoxy resin based on the diglycidyl ether of bis-phenol A cured with piperidine and containing 7 or 15% rubber toughening agent has been bonded to zinc and the adhesion measured by calculating the critical strain energy release rate, G_c, from single edge notched (SEN) and tapered double cantilever beam (TDCB) specimens. The zinc has been pretreated to give surfaces ranging from relatively flat to "microfibrous" ones covered with dendrites of the metal. The microfibrous surfaces give highest values of G_c with both modified and unmodified resins. The fracture surfaces have been studied with SEM, XPS and EPMA and the failure mode related to the joint toughness.

INTRODUCTION

The role of surface topography in adhesion is complex. Rough surfaces may inhibit wetting by the adhesive and so produce low adhesion. However, under favourable circumstances, for instance if the adhesive has low contact angle and viscosity and there is extended time before setting, surfaces of complex topography can be wetted. While there are many studies reported in the literature which report lower adhesion to rough surfaces there are also well established examples of the opposite.[1]

Some interesting effects have been found in the adhesion of polyethylene applied as a hot melt coating to metals. With conventionally prepared substrate surfaces good adhesion is only obtainable under conditions which allow oxidation of the polymer during formation of

†Present address: Department of Physics, The University, Leeds.
‡To whom communications should be addressed.

the bond.[2] However, it is possible to prepare some metal surfaces with what might be termed a "microfibrous" topography, for example by producing oxide fibres or dendritic crystals of the metal a few microns in length on the surface.[3] Adhesion of such microfibrous surfaces has been shown to be independent of oxidation of the polyethylene.

The mechanism by which the microfibrous surfaces produce good adhesion appears to involve stress concentrations at the fibre tips leading to yielding and extensive plastic deformation in the polyethylene, the work done in this plastic deformation being reflected in high peel strength.[2,3]

The present work was undertaken to study the extent to which a similar toughening of a joint could be achieved with much more brittle polymers than low density polyethylene. A commonly used epoxy resin based on the diglycidyl ether of bisphenol A was chosen as a basis. This polymer itself can be toughened by incorporation of varying proportions of a dispersed carboxy-terminated butadiene-acrylonitrile rubber phase allowing changes in ductility in the same basic material to be studied. The adhesion of such toughened epoxies to conventionally prepared metal surfaces has, of course, been extensively studied.[4-8]

This paper reports the adhesion of these both modified and unmodified resins to zinc surfaces prepared with a range of types of topography. The toughness of the bonds was assayed by measuring the critical strain energy release rate G_c and the fracture surfaces characterised using scanning electron microscopy (SEM), electron probe microanalysis (EPMA) and X-ray photoelectron spectroscopy (XPS).

Two types of adhesion specimen were employed, single edged notched (SEN)[9] and tapered double cantilever beam (TDCB).[10] The SEN generally give unstable crack propagation but the test pieces are easily made and fracture surfaces readily accessible to examination by SEM and XPS. The TDCB specimens give stable crack growth and more reproducible values of G_c but the specimens are time-consuming and relatively expensive to machine. They were less frequently cut up for surface examination.

EXPERIMENTAL

Materials

The epoxy resin was diglycidyl ether of bisphenol-A (DGEBA), Epon

828 from Shell UK Ltd. For modification a carboxyl-terminated butadiene acrylonitrile rubber (CTBN) was used. Two compositions were investigated, namely 7 and 15% by weight rubber modified epoxy in addition to the unmodified resin. All the resins were cured using 5 pphr of piperidine. The metal components were mild steel (EN3) with a zinc layer of appropriate topography electro-deposited onto the bonding surface. Early tests were carried out on solid zinc components but it was found that the metal itself was yielding plastically when the loads were high.

Surface preparation

Before electroplating, the steel surfaces were polished to 600 grade SiC paper and then degreased in trichloroethane. It was found possible to produce zinc surfaces of different form depending on the plating solutions and the plating conditions. The initial studies required a relatively flat surface devoid of any microfibrous features.

This was produced using a conventional zinc sulphate-based electroplating solution at low current density.[11] The composition of the solution was

zinc sulphate ($ZnSO_4.7H_2O$)	300 g/l
sodium chloride (NaCl)	12.5 g/l
boric acid (H_3BO_3)	19 g/l
aluminium sulphate ($Al_2(SO_4)_3.16H_2O$)	19 g/l

Depending on the current density a range of topographies could be produced ranging from a relatively flat surface (200 A/m^2), Figure 1a, to a pyramidic surface (2000 A/m^2), Figure 1b. For ease of identification the former will be referred to as "flat", the latter as "pyramidic".

It was also possible to produce a "fibrous" topography in the form of zinc dendrites. The plating solution for this type of surface contained 100 g/l of potassium hydroxide in which was dissolved 0.5 g/l of zinc oxide. Electrodeposition was carried out using a current density of 130 A/m^2. It was found that a different surface was produced depending whether the dendrites were plated straight onto a clean steel surface or whether a thin coat of zinc was first plated using the zinc sulphate solution at 200 A/m^2. Plating straight onto steel gave a partially dendritic surface, Figure 2a, while plating a thin coat of zinc first, produced a fully dendritic surface, Figure 2b.

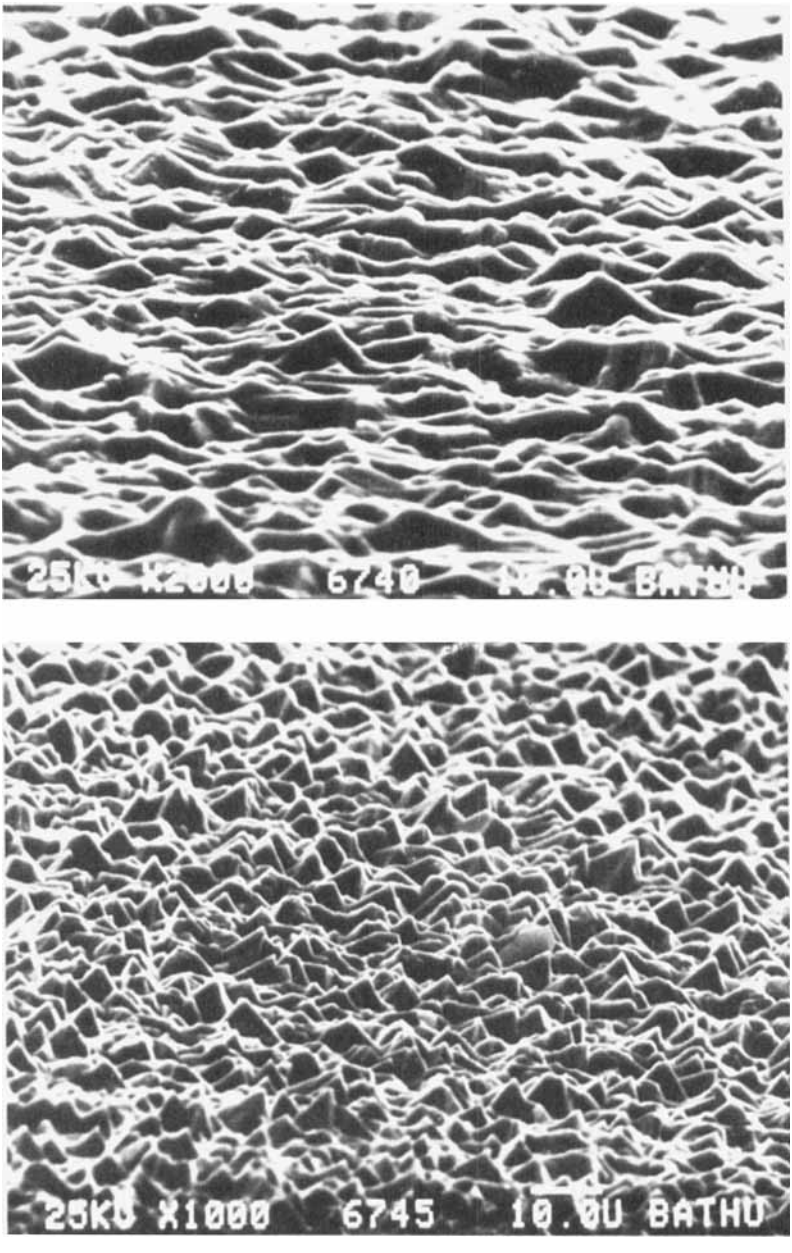

FIGURE 1 SEM photographs of surface of zinc electrode deposited from zinc sulphate based solution (a) "flat" surface formed at 200 A/m^2 (b) pyramidic surface formed at 2000 A/m^2.

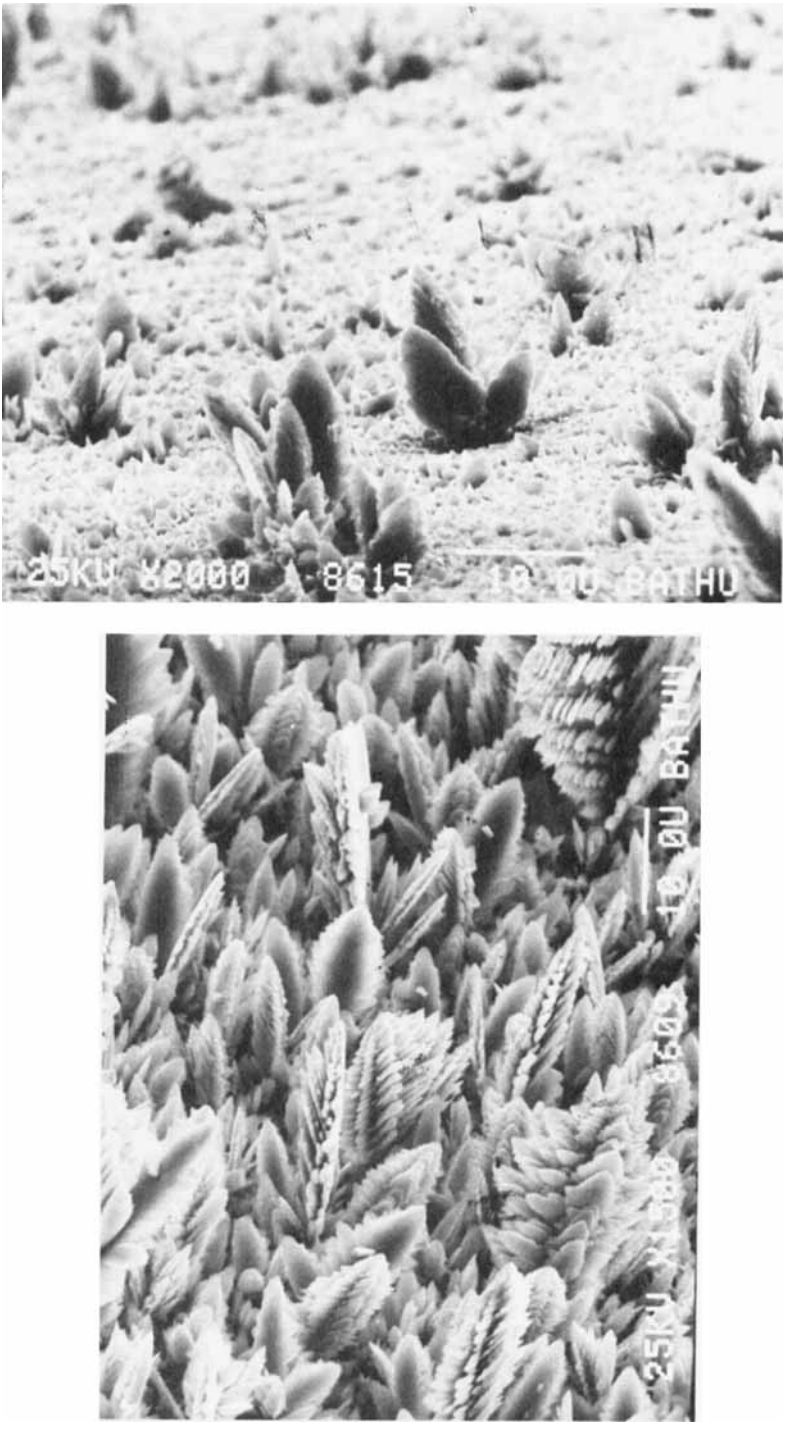

FIGURE 2 SEM photographs of surface of zinc electrode deposited from potassium hydroxide based solution (a) partially dendritic. (b) fully dendritic surface. (Scale bars represent 10 μm).

Preparation of the Joints

Two specimen geometries were used to study the adhesive properties of the various systems. The single edge notch test is shown schematically in Figure 3. Typical dimensions for an SEN specimen were 20 mm wide (W), 5 mm thick (B) and 100 mm long. The crack lengths used for testing were generally between 8 and 12 mm. One half of the sample was metal with one surface suitably prepared as has previously been described. A piece of PTFE tape 0.07 mm thick was glued over half of the prepared surface to give an initial starting crack at the interface. The resin to be used was then cast against the prepared surface in a silicone rubber mould (RTV-700 Silicone flexible mould rubber—Alec Tiranti Ltd). If the resin was to be modified the resin and rubber were heated separately to 80°C to aid the mixing of the two phases. After mixing the solution left, again at 80°C, for all bubbles to disappear before adding the curing agent. The curing schedule for both the epoxy and the rubber modified resin was 16 hours at 120°C.

The tapered cantilever beam test specimen is shown in Figure 4. A narrow taper of 7° was chosen[10] in preference to a contoured beam as a consequence of the former being simpler and quicker to produce in any quantity. The thickness of the metal substrates was 12.4 mm, the surfaces to be bonded being prepared as previously described. The thickness of the ahesive layer was controlled using appropriate brass shims most of the work being done on 0.14 mm bonds. A piece of PTFE tape thickness 0.07 mm was placed at the narrow end of the joint to assist the initial crack propagation. The resin, mixed as previously explained, was then applied to one of the bonding surfaces and then the substrates were clamped together at each end. Plastic tape was pressed onto one side of the bond to keep the resin in the gap during curing. The whole system was then placed in the oven and cured for the same cycle as that for the SEN samples. After curing, both types of specimen were cleaned to ensure no epoxy overlapped the metal surfaces which might have provided extra adhesion on testing. In both cases this meant polishing the epoxy until it was flush with all metal surfaces. The samples were then ready for testing.

Testing of the samples

Both types of specimen were tested in tension on an instron testing machine at a crosshead displacement rate of 0.2 mm/min. For the

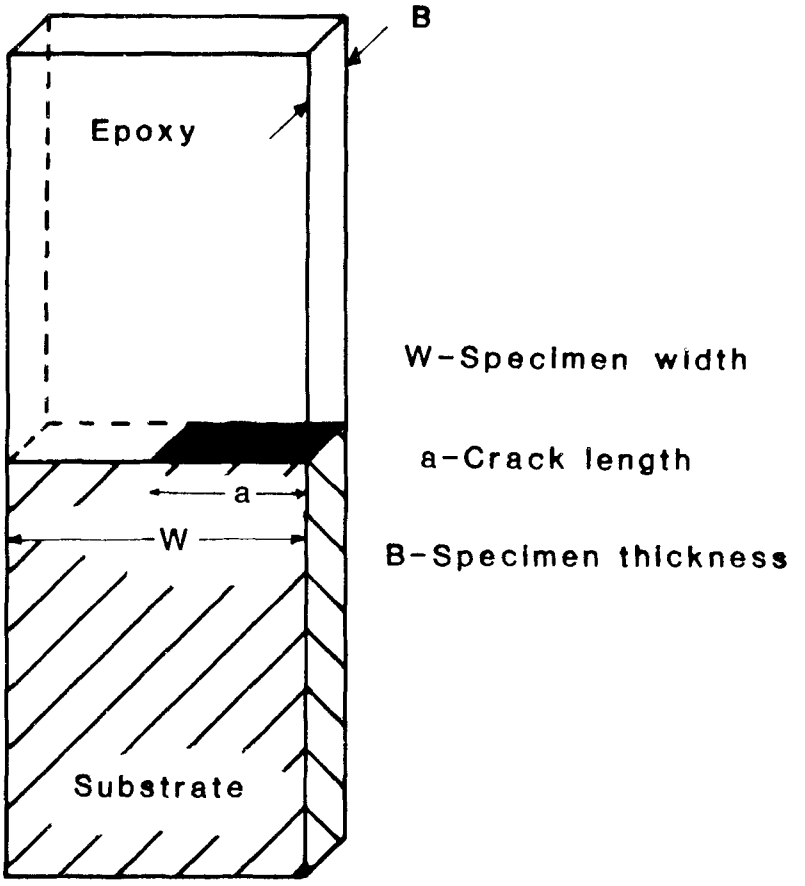

FIGURE 3 Single edge notch (SEN) adhesion specimen. Precrack shown in solid black.

SEN test the fracture was generally of an unstable nature, the initiation load being used to calculate the value for the critical plane strain energy release rate G_c.

Williams[12] has discussed the application of conventional fracture mechanics test pieces to the measurement of adhesion. Formulae similar to, but not identical with, those appropriate for a single phase specimen can be used for adhesion specimens. Thus in this work G_c for the SEN specimens was calculated using the equation given

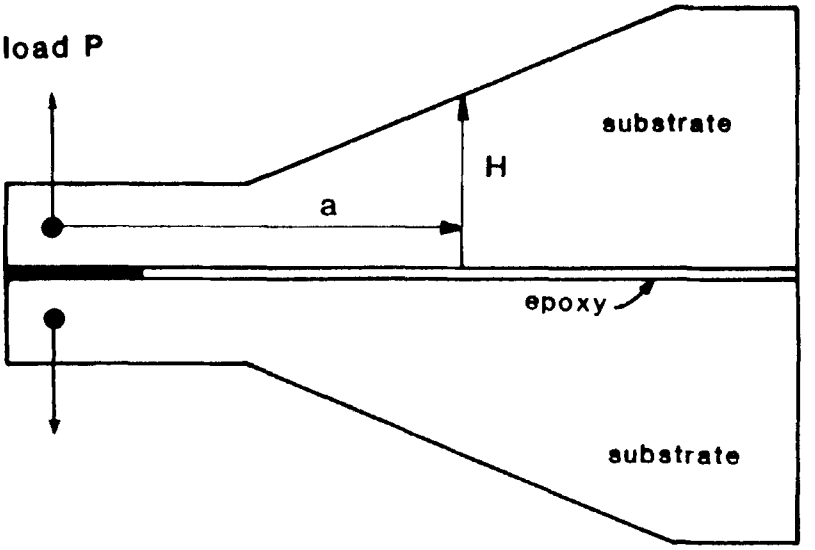

FIGURE 4 Tapered double cantilever beam (TDCB) adhesion specimen. Precrack shown in solid black.

by Brown and Srawley[13] modified by the introduction of a factor of a half as justified by Williams:

$$G_c = P^2a[2B^2W^2E^*]^{-1}[1.99–0.41(a/W) + 18.7(a/W)^2 – 38.48(a/W)^3 + 53.85(a/W)^4]^2$$

where E^* = plane strain modulus
P = fracture load

and the other symbols are defined in Figure 3.

For the TDCB both stable and unstable fracture modes were encountered. In both cases it was necessary to note the crack length, as it propagated along the adhesive bond with respect to the load/deflection graph, in order to calculate a value of G_c. This was done at intervals of 1 cm along the fracture path. An average value of G_c was then calculated for each sample. The equation for G_c was taken from the work of Srawley and Gross[14] and is given by

$$G_c = P^2a^2[B^2H^3E_s]^{-1}[3.26 + 2.828(H/a)]^2$$

where P = fracture load; B = substrate thickness; E_s = substrate modulus.

The other parameters are as shown in Figure 4. This method of analysis has a slightly different emphasis from that employed by workers using a contoured tapered cantilever beam.[10] The shape of the contoured beam is such that the compliance is independent of crack length and so no measure of crack length is needed during the test.

Surface analysis

After failure the two fracture surfaces were examined by a number of techniques. Firstly an examination was carried out using a scanning-electron microscope, in this case a JEOL JSM 35C. In order to examine the surfaces in the SEM the appropriate surfaces were removed from the substrates by carefully sawing out the relevant section. Subsequently an investigation was carried out into the locus of failure using electron probe microanalysis and x-ray photoelectron spectroscopy. The EPMA was carried out using an EDAX 9100 system. The technique had a sampling depth of the order of 1μm and was used to examine surfaces which had a mixture of cohesive and adhesive failure. Mostly the technique was used to investigate the epoxy side of the failure in order to see if any zinc had been left in the polymer side of the fracture plane. The XPS spectra were taken with a KRATOS ES300 electron spectrometer using MG Kα x-rays (E_{x-ray} = 1253.6 eV). The sampling depth of the technique was of the order of 30Å and so was much more surface sensitive than EMPMA. It was employed exclusively to check the apparent adhesive failures to ascertain whether truly adhesive failure occurred.

RESULTS

Tapered double-cantilever beam specimens

Experiments were done with these specimens at the two extremes of surface topography, "flat" and fully dendritic. The results given in Table I refer to the standard bond thickness of 0.14 mm. Except for the case mentioned below, the crack propagated stably at a velocity of about 3 cm/min.

Unmodified Epoxy Resin. With the "flat" zinc surface the un-

TABLE I
Adhesion of epoxy resin to zinc. Critical strain energy release rate G_c values (J/m^2) for TDCB specimens of different surface topography. Bond thickness 0.14 mm.

Rubber modification	Flat zinc	Fully dendritic zinc
0	140 ± 45	205 ± 75
7	1465 ± 500	2540 ± 180
15	1900 ± 150	3400 ± 540

modified resin gave a stable fracture and a low value of G_c. The fracture path was close to the zinc surface. In the SEM no residual polymer was observed on the zinc surface and the epoxy side of the fracture surface, which closely resembled Figure 1a, appeared to be a faithful replica of the topography of the metal with no signs of plastic deformation.

This evidence on its own would suggest that the failure was adhesive, *i.e.* at the substrate polymer interface. However, the zinc side of the fracture surface was examined by XPS and compared with the spectra of the unbonded zinc and of the resin itself. Figure 5 shows a typical comparison for the oxygen 1s region between the unbonded zinc surface, the unmodified resin and the metal surface after failure. The peak due to ether linkages in the resin[15] is at a lower binding energy than that due to the oxygen species on the unbonded metal. The spectrum of the metal side of the fracture is seen to be broader than the unbonded metal surface due to the ether contribution from the polymer. This piece of information is part of an overall picture which includes spectra from the carbon and zinc regions.

The unbonded zinc surface gave a carbon 1s spectrum caused by contamination which is always found under such experimental circumstances.[16] Compared with this the C1s spectrum of the resin has a pronounced shoulder on the high binding energy side of the main (hydrocarbon) peak. The shoulder is associated with the carbon bonded to oxygen in ether groups in the resin.[15,16] The C1s spectrum of the fracture surface showed this feature although to a smaller extent than the resin itself. The zinc $2p^{3/2}$ peak was present on the fracture surface but less intense than on the unbonded metal. Thus it appears that there is a thin layer of epoxy resin on the fracture surface which is not visible in the SEM.

The zinc signal might have come from the substrate under the epoxy layer in which case the polymer must be less than about 30A thick.[17] Alternatively the zinc signal might result from isolated areas

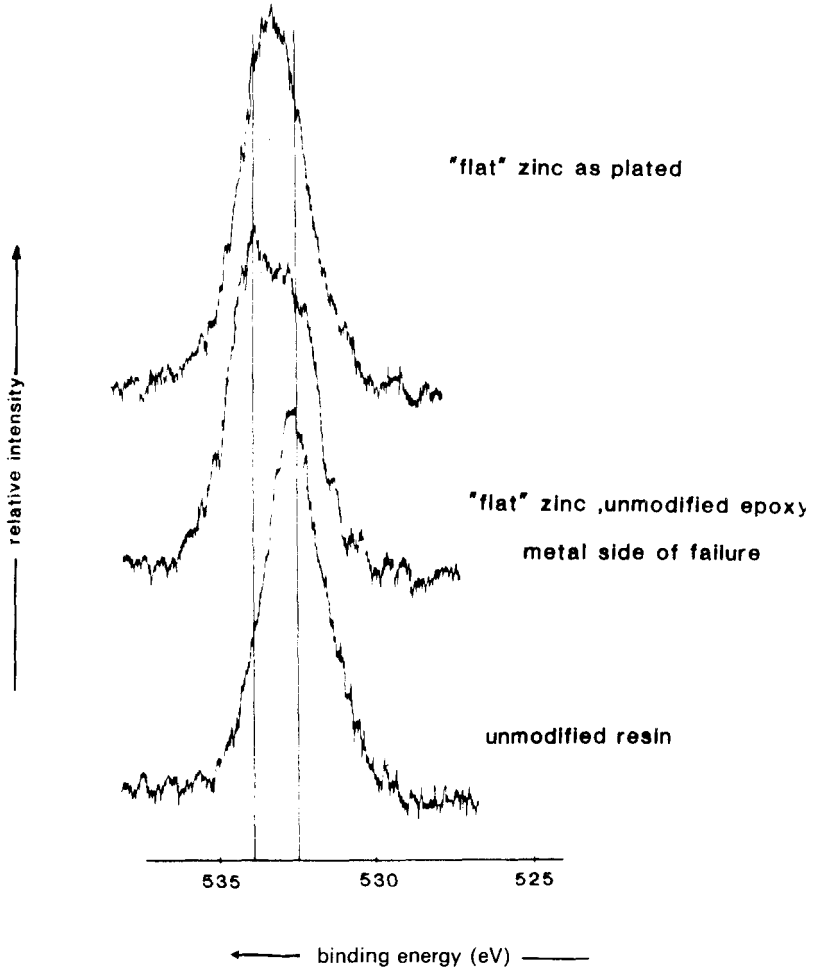

FIGURE 5 01s XPS spectra of "flat" zinc surface, unmodified epoxy resin and metal side of the fracture between the "flat" zinc and unmodified resin.

of adhesive failure in a fracture path which otherwise passes through the resin close to the interface. Gettings, Baker and Kinloch have suggested that such a mode of failure occurs in epoxy steel joints.[18]

With a fully dendritic surface (Figure 2b) the unmodified resin gave a significantly higher value of G_c (Table 1). The crack travelled across the sample in a series of jumps. This type of failure, known as "stick-

slip", has often been observed in similar systems and its causes discussed by various authors.[5,6,19,20] The values of G_c in Table I are calculated from peak loads, *i.e.* they refer to initiation rather than to arrest of the crack. The locus of failure for this category of joint was cohesive in the resin. The failure was well away from either interface near the centre of the bond.

Rubber modified epoxy resin. For the "flat" zinc there was a small increase in toughness in going from the seven to the fifteen per cent rubber modified epoxy resin (Table I). In both cases the polymer appeared stress whitened throughout the bond thickness. Although the SEM revealed occasional small pieces of resin on the zinc side of the fracture surface no resin was visible over the majority of the surface although a thin layer may have been present as was the case with the unmodified resin. The resin side of the fracture showed no evidence of plastic deformation of surface region.

For the fully dendritic surface there was a significant increase in G_c for both rubber additions and by a similar percentage in each case. The polymer was again fully stress whitened, the fracture path appearing to pass through the resin but close to the dendrite tips. Both sides of the fracture surface showed widespread plastic deformation (Figure 6). It is significant that thicker bond lines produced higher values of strain energy release rate (Table II).

Single edge notched specimens

The full range of surface topographies was studied using this type of specimen. The results are shown in Table III. In this test configuration the crack propagation is usually unstable so that value of G_c obtained is particularly sensitive to the initial notch. Thus the scatter for the SEM results tends to be higher than that obtained for TDCB specimens.

Care also has to be taken when interpreting the fracture surfaces as what happens after initiation may not be completely compatible with the toughness values obtained from this instability point. However, when such care is taken the surface analysis can give valuable information in interpreting the trends that were seen.

Most of the fracture surfaces showed a mixture of cohesive and apparently adhesive failure, the amount of residual polymer increasing with toughness of the bond.

Unmodified Epoxy Resin. The "flat" zinc surface gave a low value

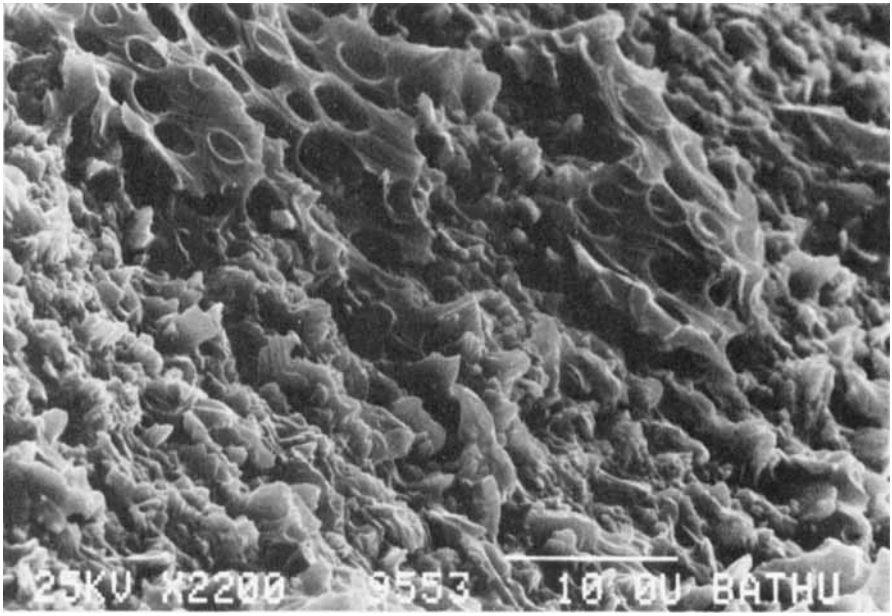

FIGURE 6 SEM of the metal side of the fracture surface for 15% rubber modified epoxy resin bonded to a fully dendritic zinc surface in TDCB specimen. Plastic deformation is visible in the residual layer of resin. (Scale bar represent 10 μm).

TABLE II
Effect of bond thickness on critical strain energy release rate G_c for TDCB specimens with dendritic zinc surfaces bonded with epoxy resin with 15% rubber modification

$G_c(J/m^2)$	Bond thickness (mm)
3403 ± 542	0.14
4400 ± 750	0.25
5100 ± 700	0.45

of G_c (Table III). XPS investigation of the zinc side of the fracture surface gave evidence of the presence of resin which did not completely obscure the zinc photoelectrons. No epoxy could be seen in the SEM. Thus the mode of failure was similar to that of the corresponding TDCB specimens, a very thin layer of epoxy remained possibly with islands of adhesive failure exposing the substrate surface.

The pyramidic zinc surface (Figure 1b) gave a similar failure mode

TABLE III
Critical strain energy release rate (G_c) values (J/m^2) for SEN specimens of different surface topography

Substrate	G_c	Fracture mode
Epoxy resin		
Flat zinc	105 ± 30	Apparently adhesive, thin layer polymer (< 30A)
Pyramidic zinc	135 ± 75	Adhesive. Small areas of polymer on metal side ($\approx 1\mu m$)
Partially dendritic zinc	305 ± 175	Adhesive. Small areas of polymer on metal side ($\approx 1\mu m$)
Fully dendritic zinc	670 ± 290	Cohesive. Fracture path above dendrite tips
7% Rubber modified expoxy		
Flat zinc	295 ± 110	Adhesive with small residual polymer areas
Fully dendritic zinc	2210 ± 900	(Cohesive. Most of the resin on the metal side. Some stress whitening)
15% Rubber modified epoxy		
Flat zinc	700 ± 200	Adhesive with residual polymer areas ($\approx 10\mu m$)
Pyramidic zinc	766 ± 365	Adhesive/Cohesive. Large areas of polymer ($\approx 100\mu m$)
Partially dendritic zinc	2400 ± 730	Adhesive/Cohesive. Large areas of polymer on metal side ($\approx 100\mu m$)
Fully dendritic zinc	2548 ± 515	Cohesive. Most resin on metal side

and a modestly higher value of G_c (Table III). The partially dendritic surface (Figure 2a) presented some interesting features. The load-displacement characteristic was different from that shown by any of the other categories of SEN specimens investigated in this work. When the load reached a critical value, crack propagation was stable in the sense that continuous further cross head movement was necessary for further propagation of the crack through the specimen (Figure 7). The value of G_c (calculated from the initiation point) was considerably higher than that for the "flat" and pyramidic surfaces previously discussed (Table III). As the crack propagation was stable an alternative method for calculating G would be from an energy balance approach. In its simplest form this considers the crack propagation in terms of the rate of change of the system energy U with crack extension a. The strain energy release rate G is then defined as

$$G = \frac{-1}{B}\left(\frac{\partial U}{\partial a}\right)$$

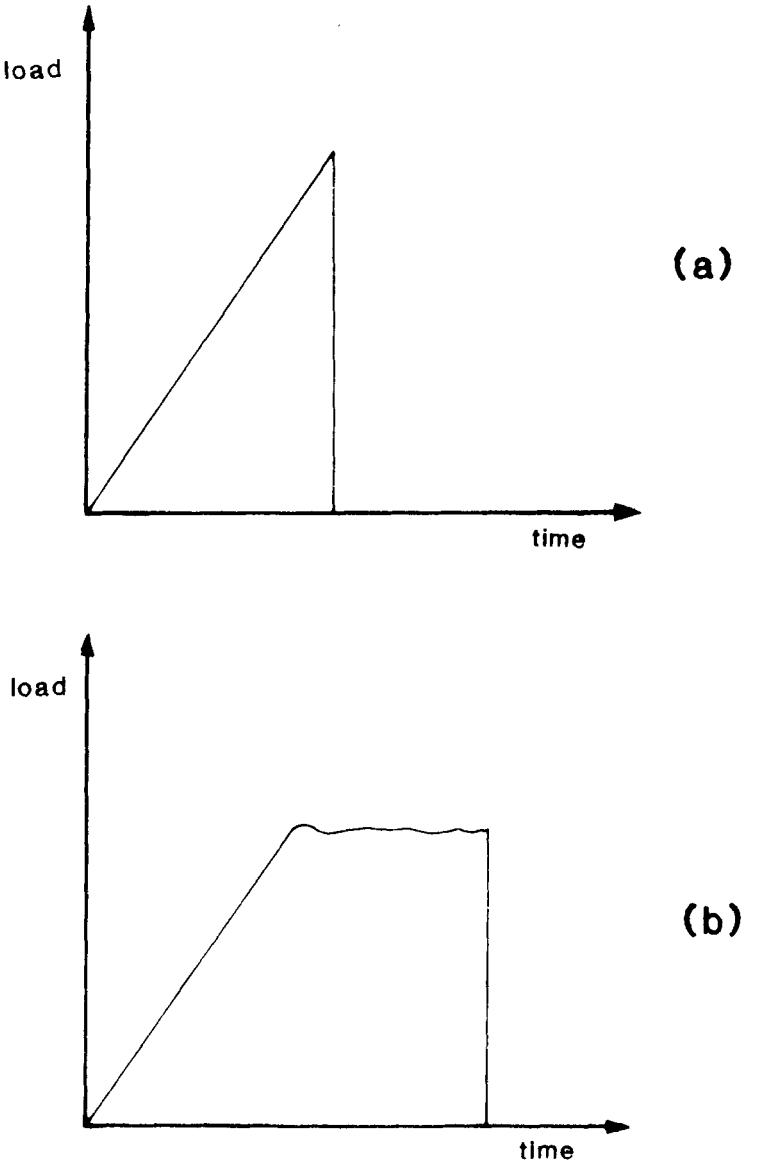

FIGURE 7 Schematic representations of load-time graphs for SEN test (a) unstable crack propagation most commonly found. (b) Stable crack propagation found only for partially dendritic zinc bonded to unmodified epoxy resin.

for a body of thickness B.

Analysing the load deflection diagrams for the partially dendritic surfaces in this way gave a value for G of 390 ± 75 J/m^2 which is now a stable propagating value. This is not too different from the instability value calculated.

The failure mode for the partially dendritic surfaces was also unusual. In the SEM a few scattered islands of resin could clearly be seen on the substrate surface but the major part of the area resembled the original zinc surface except that none of the dendrites (see Figure 2a) were to be seen. This suggested that they had been stripped

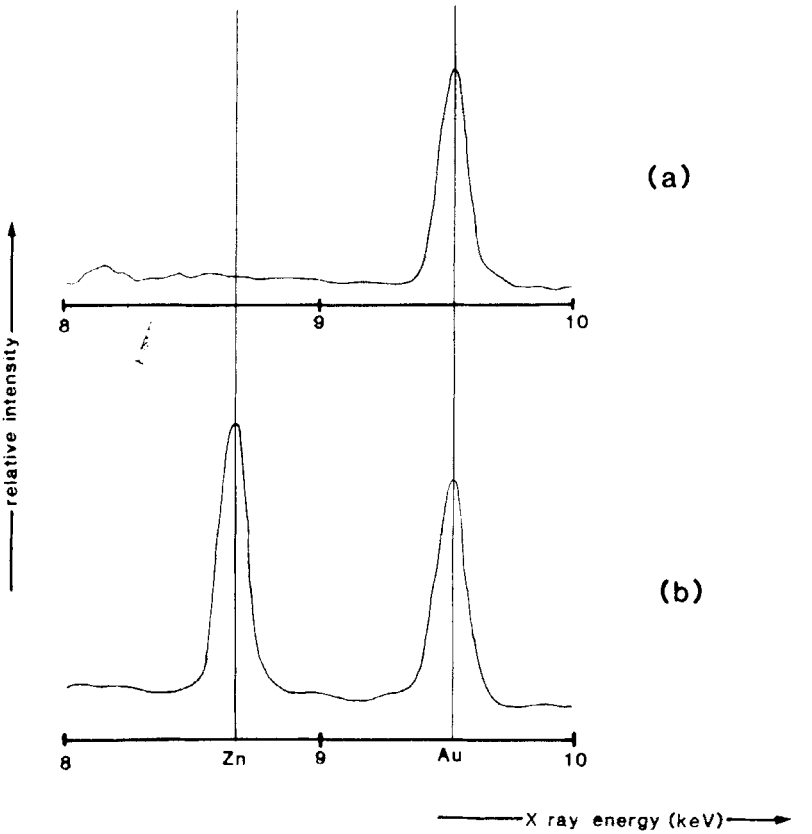

FIGURE 8 EPMA spectra of the resin side of the fracture between unmodified epoxy resin and zinc SEN specimens (a) "Flat" zinc showing only the signal from the gold coating applied (b) Partially dendritic zinc showing the presence of zinc in the resin.

off and were still embedded in the resin. Investigation of the epoxy side of the fracture surface by EPMA indicated the presence of considerable quantities of zinc (Figure 8) supporting this interpretation.

For the fully dendritic surface the toughness is still further increased (Table III). Failure was cohesive in the resin just above the tips of the dendrites (Figure 9). In some places the tips were visible in the SEM. The surface of the resin shows plastic deformation.

Rubber modified epoxy resin. As was found for the TDCB tests, the modified resin gave higher values of G_c and somewhat less scatter (Table III). It can be seen that there is a much greater percentage improvement in the toughness by using a fibrous topography compared with the TDCB test. This is a consequence of the bond constriction effect in the TDCB test giving an increase in toughness even for the "flat" zinc surface.

For all the surfaces it was found that the value of G_c for the 7 per

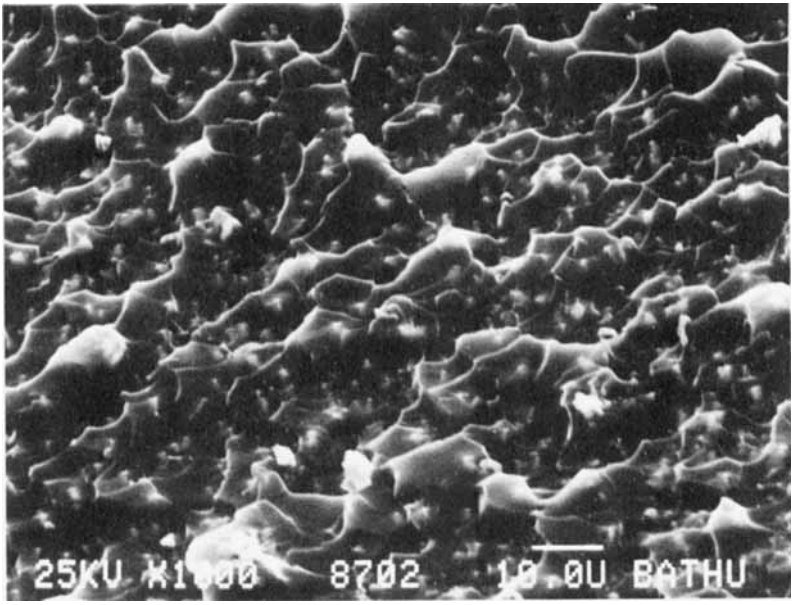

FIGURE 9 SEM of the substrate side of the fracture of a SEN specimen of fully dendritic zinc bonded to unmodified resin. The dendrite tips are clearly visible just below the surface (scale bar represents 10 μm).

cent rubber modified epoxy laid between the unmodified epoxy and the 15 per cent rubber modified epoxy. For the "flat" zinc surfaces the metal side of the failure had quite large (*ca.* 10μm) pieces of resin adhering. There were also apparently adhesive regions which again could of course have a thin polymer layer on the surface.

The pyramidic surface, investigated for the 15 per cent rubber toughened resin only, showed little improvement in toughness compared to the "flat" zinc although the areas of residual polymer visible on the substrate tended to be somewhat larger.

The partially dendritic surface, again for the 15 per cent rubber toughened resin, once more provided interesting results. The value of G_c was high (Table III) and a significant proportion of the substrate fracture surface was covered with residual polymer (Figure 10). No dendrites could be seen in the areas where resin appeared absent. Again EPMA detected zinc in the resin fracture surface.

The fully dendritic surface was tested for both rubber toughening additions and gave a high value of G_c. The value for the 15 per cent rubber modified resin was of a similar magnitude to that from the partially dendritic surface. The locus of failure in both cases was in the resin, the dendrite tips causing widespread deformation of the polymer (Figure 11). The polymer was stress whitened on both sides of the fracture plane.

DISCUSSION

The two types of test specimen give broadly similar failure modes and relative values for G_c for corresponding combinations of polymer and surface topography (Table I and III). The difference between the absolute values of G_c for the SEN and TDCB specimens follows from the different test geometry. In the SEN the stress is concentrated at the interface and so the effect of surface geometry is more pronounced. Similarly, the crack propagation tends to be stable in the TDCB but unstable in the SEN specimens leading to a greater notch sensitivity.

There is a considerable literature on the adhesion of epoxy resins to metals, particularly aluminium and steel. The question of the chemical nature of the bond between the oxidised surface of the metal and the resin has exercised a number of authors. Several earlier authors supported various schemes for chemical bonding, particularly for aluminium and steel.[21,22,23] More recent papers on the bonding to aluminium[24] and to steel[25] concluded that no primary bonds were in-

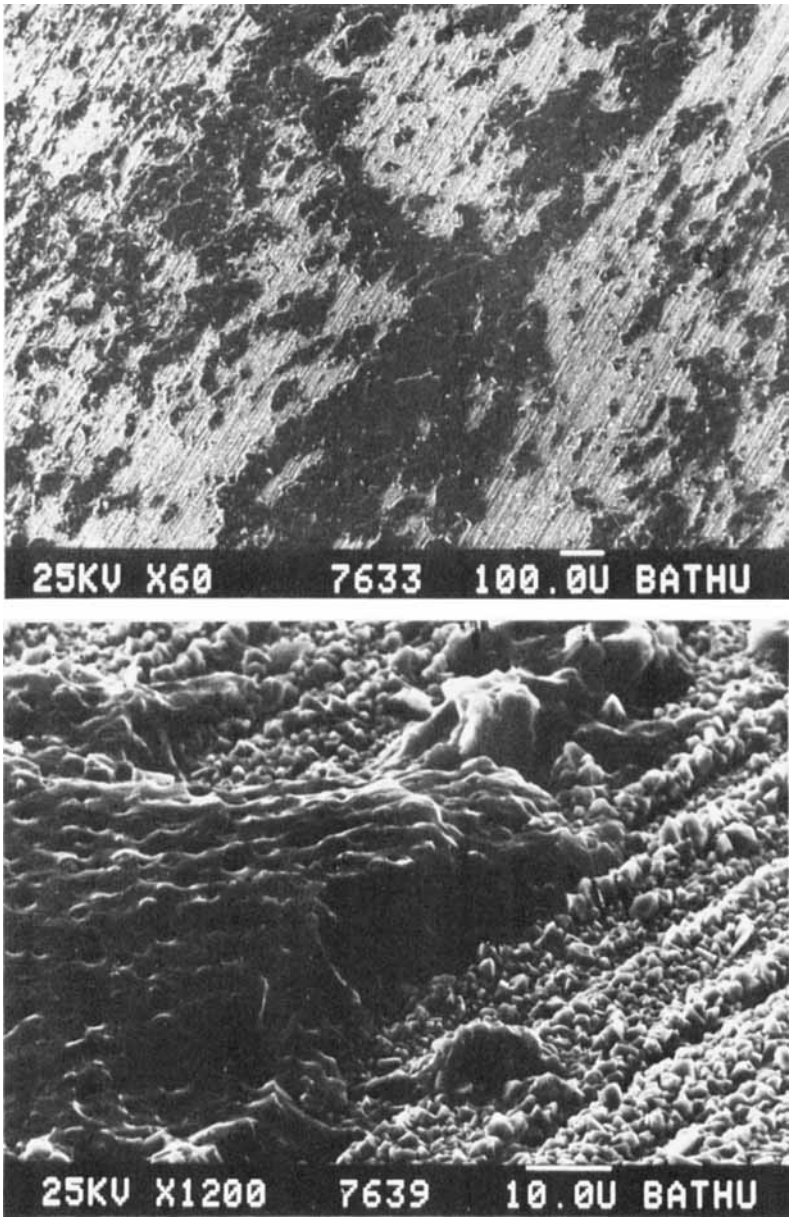

FIGURE 10 SEM of the substrate side of the partially dendritic zinc surface bonded to 15% rubber modified epoxy resin in a SEN specimen. (a) Overall view showing extensive areas of residual polymer and regions of apparently bare zinc (Scale bar 100 μm) (b) High magnification view of the border between the two regions (Scale bar 10 μm).

FIGURE 11 SEM of substrate side of fully dendritic zone bonded to 15% rubber modified epoxy resin in a SEN specimen (Scale bar 10 μm).

volved. Andrews found indirect evidence of primary bonding to titanium[26] but only of secondary bonds where aluminium, steel or gold were involved as long as stoichiometric resin-hardener ratios were used.[27] The unmodified resin- "flat" zinc combination serves as a sort of datum in this work. The G_c value (Table I) is lower than those found elsewhere for epoxy bonded to steel, aluminium or copper,[5,28,29] so there is no reason for postulating primary bond formation in this case. Whether or not this is correct it seems unlikely that altering the topography of the zinc would significantly affect the nature of the chemical interaction with the polymer. The explanation of the increases in G_c which these changes produce must be sought in other terms.

The presence of the rubber phase causes a large increase in toughness of the joint (Table I and III) as reported in many other papers.[4-8] The rubber particles lower the yield stress of the resin, increase the plastic zone size and so make it much more ductile. This enhanced plasticity is manifested by the stress-whitened appearance of the deformed resin. The higher adhesion of this material to the "flat" zinc then is a consequence of the lower yield strength enabling much of the resin itself to yield plastically, absorbing energy and increasing G_c. The value of G_c depends on the volume of resin which can deform plasticially and stress whiten under the test conditions. For the TDCB specimen this is limited by the bond thickness. For thicker bonds greater stress whitening and higher G_c values are found (Table II). This effect for conventionally prepared surfaces is well documented.[5,6,8]

The influence of substrate topography is the principal theme of this work. The main contrast is between the two extremes: the "flat" and fully dendritic surfaces. For both surfaces extensive stress-whitening of the rubber-modified resin was visible to the naked eye. No difference in appearance of the stress-whitened areas from the different substrates could be seen in the SEM. The obvious effect of the dendrities was to move the locus of failure to the region of the dendrite tips and to cause extensive plastic deformation of the resin on both sides of the fracture surface. This is reminiscent of the failure mode found between low density polyethylene and surfaces with microfibrous topography.[3] It seems likely then that the increased energy dissipation with the modified resin bonded to the fully dendritic surface is associated with additional plastic deformation of the resin along the fracture plane and that this is the result of stress concentration at the dendrite tips.

It is interesting that even with the much more brittle unmodified resin the dendrites compared with the "flat" surface exert a toughening effect. The effect is more dramatic with the SEN specimens where the stress is concentrated at the interface. G_c for the fully dendritic surface is similar to that for the 15% rubber modified resin bonded to "flat" zinc (Table III). The SEM gives indications of the reasons for the additional toughening of the unmodified resin (Figure 9). The surface consists of a series of hollows and ridges: some of the latter show sign of limited plastic deformation. The presence of fibre tips first beneath the centres of some of the hollows suggest that these may have acted as sites of initiation in addition to the preformed crack. It is significant that at the magnification on Figure 9 the fracture surface of a cohesive SEN specimen of the resin itself is completely smooth. Kinloch *et al.*,

have discussed effects of rate and temperature on transitions from brittle to ductile failure in such resins and on the appearance of the corresponding fracture surfaces.[30] In the present work it is seen that a transition from brittle to ductile behaviour can be produced by change of substrate topography.

Of the two intermediate surface topographies which were investigated with SEN specimens, the pyramidic surface only produced a slight increase in G_c. This may be associated with the modest increase in surface area.

The partially dendritic surfaces gave rise to some interesting features. With the unmodified resin the failure was close to the original zinc surface except that the dendrites had been stripped off and were embedded in the resin. This suggests that the higher G_c compared with the flat surface must be associated with the energy involved in fracturing the dendrites and the associated straining of the resin around them. With the 15% modified resin some areas of fracture were like this, others resembled that of the fully dendritic surface. With the more ductile resin the partially dendritic surface produces enough stress concentration for bulk yielding so the value of G_c was practically the same as for the fully dendritic surface.

CONCLUSIONS

Broadly similar trends have been found for the adhesion of epoxy resins to zinc using both SEN and TDCB test specimens. The adhesion increases with the proportion of rubber phase incorporated in the epoxy but the extent to which the toughening potential of the modified epoxy is realised depends upon the topography of the surface. The more complex the surface topography, the higher the value of G_c produced. It is interesting that even with the more brittle unmodified resin a useful increase in G_c can be obtained in changing from a "flat" to fully dendritic surface.

The fracture surfaces for high and low G_c are characteristically different. For low G_c they are relatively smooth but for high G_c considerable plastic deformation is shown by both modified and unmodified polymers. High toughness is associated with plastic deformation of the surface and, for the modified resins, stress-whitening in the bulk. In some cases a contribution comes from fracturing dendrites on the zinc surface.

Acknowledgements

The support of the SERC for this work and in the provision of electron optical facilities at Bath are gratefully acknowledged. Thanks are also due to Professor D. T. Clark of the University of Durham for access to the x-ray photoelectron spectrometer.

References

1. D. E. Packham, *Adhesion Aspects of Polymeric Coatings*, K. L. Mittall, Ed. (Plenum, New York, 1983). p. 19.
2. D. E. Packham, *Developments in Adhesives-2*, A. J. Kinloch. Ed. (Applied Science, London, 1981). p. 315.
3. J. R. G. Evans and D. E. Packham, *J. Adhesion*, **10**(3), 177 (1979).
4. A. C. Meeks, *Polymer*, **15**, 675 (1974).
5. W. D. Bascom, R. L. Cottington, R. L. Jones and P. Peyser, *J. App. Polym. Sci.*, **19**, 2545 (1975).
6. W. D. Bascom and R. L. Cottington, *J. Adhesion*, **7**(4), 333 (1976).
7. C. B. Bucknall and T. Yoshii, *B. Polym. J.* **10**, 53 (1978).
8. A. J. Kinloch and S. J. Shaw, *J. Adhesion*, **12**(1), 59 (1981).
9. A. N. Gent, *Rubb. Chem. Technol.*, **47**, 202 (1974).
10. E. J. Ripling, S. Mostovoy and H. T. Corten, *J. Adhesion*, **3**(2), 107 (1971).
11. E. A. Ollard, *Introductory Electroplating* (Wiley and Sons, New York, 1969).
12. M. L. Williams, *J. Adhesion*, **4**(4), 307 (1972).
13. W. F. Brown and J. E. Srawley, *Plane Strain Fracture Toughness Testing*, ASTM, Sp. Tech. Publ. 410 1966.
14. J. E. Srawley and B. Gross, *Stress Intensity Factors for Crack-line-loaded Edge Crack Specimens*, NASA TN D3820 (1967).
15. J. F. Watts, PhD Thesis, University of Surrey, 1983.
16. D. T. Clark, *Polymer Surfaces* D. T. Clark and W. J. Feast Eds (Wiley, New York, 1978). p. 309.
17. D. M. Wyatt, R. C. Gray, J. C. Carver, D. M. Hercules and L. W. Masters, *App. Spectroscopy*, **28**, 439 (1974).
18. M. Gettings, F. S. Baker and A. J. Kinloch, *J. Appl. Polym. Sci.*, **21**, 2375 (1975).
19. S. Mostovoy, E. J. Ripling and C. F. Bersch, *J. Adhesion* **3**(2), 125 (1971).
20. R. A. Gledhill and A. J. Kinloch, *Polymer* **17**, 727 (1976).
21. N. A. de Bruyne, *J. Appl.* Chem., **6**, 303 (1965).
22. H. Alter and W. Soller, *Ind. Eng. Chem.*, **50**, 922 (1958).
23. G. J. Barenholtz, I. C. Chu and J. E. Rutzier, Preprints ACS Div. Paint, Plastics, Printing Ink, **20**(1), 117 (1960).
24. J. P. Bell and W. T. McCarvill, *J. Appl. Polym. Sci.*, **18**, 2243 (1974).
25. R. A. Gledhill and A. J. Kinloch, *J. Adhesion*, **6**(4), 315 (1974).
26. E. H. Andrews and A. Stevenson, *J. Adhesion*, **11**(1), 17 (1980).
27. E. H. Andrews and N. E. King, *J. Mat. Sci.*, **11**, 2004 (1976).
28. S. Yamini and R. J. Young, *Polymer*, **18**, 1075 (1977).
29. P. J. Hine and D. E. Packham, to be published.
30. A. J. Kinloch, S. J. Shaw, D. A. Tod and D. L. Hunston, *Polymer*, **24**, 1314 (1983).